Research Article

A thermodynamic database of the Ni-Mo-Re system

Xiong-Hui Lei[1], Wei Liu[2], Fenghua Luo[3], Xiao-Gang Lu[1,2,*]

[1]School of Materials Science and Engineering, Shanghai University, Shanghai 200444, China.
[2]Materials Genome Institute, Shanghai University, Shanghai 200444, China.
[3]State Key Laboratory of Powder Metallurgy, Central South University, Changsha 410083, Hunan, China.

*Correspondence to: Prof. Xiao-Gang Lu, School of Materials Science and Engineering, Shanghai University, No. 333 Nanchen Road, Shanghai 200444, China. E-mail: xglu@t.shu.edu.cn

Abstract

Thermodynamic databases are essential prerequisites for developing advanced materials, such as Ni-based superalloys. The present work collects a large amount of experimental and first-principles calculation data concerning the thermodynamics and phase diagrams of the Ni-Mo-Re system, based on which the thermodynamic properties of the ternary and its binary sub-systems Ni-Mo and Mo-Re are assessed by means of the CALculation of PHAse Diagrams (CALPHAD) approach. The thermodynamic database containing all model parameters is established and most experimental data are reproduced satisfactorily. The present work demonstrates the use of the CALPHAD method as a practical appliance in the toolbox of materials informatics to analyze and discriminate various types of data by thermodynamic modeling and then produce more useful data in wider ranges of compositions and temperatures by computational predictions.

Keywords: Ni-Mo-Re, first-principles calculations, thermodynamic modeling, CALPHAD

INTRODUCTION

Ni-based superalloys play a significant role in high-temperature applications for modern industry[1]. Refractory alloying elements, such as Mo and Re, are often added to enhance the high-temperature performance of Ni-based superalloys further. However, some harmful brittle topologically close-packed (TCP) phases may form with increasing contents of alloying elements. In order to understand the phase stabilities of TCP phases,

as well as their equilibria with other phases, it is necessary to develop a reliable thermodynamic database to predict phase equilibria and transformations in Ni-based superalloys, starting from ternaries, such as Ni-Mo-Re.

The phase diagram and thermodynamics of the Ni-Mo-Re ternary system were studied by Yaqoob and Joubert[2,3] and the enthalpies of formation of compounds were calculated by Crivello[4] by means of first-principles calculations. A new phase with a modulated σ phase structure was reported and named as the σ' phase by Yaqoob *et al.*[5]. The average structure of this phase is the σ phase, existing in the binary Mo-Re system and extending to the ternary Ni-Mo-Re system. Further structural characterization of this compound could not be completed because of the poor quality of the sample. Yaqoob[2] treated the phase as a line compound, $(Mo,Re)_2(Ni)_1$, without considering its structural relationship with the σ phase and ignoring the experimentally determined solubility range of Ni from ~26 to ~33 at.%. There exist other limitations in the assessment by Yaqoob[2] regarding the subsystems, the extension of the binary δ phase in the ternary system and the liquidus projection.

The present work aims to obtain a set of self-consistent thermodynamic parameters of the Ni-Mo-Re system with more inputs from first-principles calculations. The binary systems Ni-Mo and Mo-Re are revised to obtain a better agreement with the experimental data. By combining the thermodynamic description of the Ni-Re system reported by Yaqoob and Joubert[6] with the updated Ni-Mo and Mo-Re systems, the reassessment of the Ni-Mo-Re ternary system is carried out.

LITERATURE REVIEW

All available experimental studies[3,7–46] are summarized in Table 1.

Ni-Mo

The Ni-Mo system has been extensively investigated by experiments[3,7–33] and thermodynamic modeling[32,33,47–49]. Due to the lack of experimental and first-principles calculated thermodynamic data, earlier thermodynamic assessments[47,48] are less reliable considering the formation enthalpies of some intermetallic compounds. Morishita *et al.* treated the δ phase as a stoichiometric compound, which is inconsistent with the homogeneity domain of 4 at.%[49]. With the aid of first-principles calculations (some of the data were calculated by Wang *et al.*), Zhou *et al.* obtained a set of thermodynamic parameters of the Ni-Mo system by the CALPHAD method[31,32]. However, overfitting with too many parameters to the phase diagram at low temperatures led to a much larger heat capacity (C_P) deviation from the experimental data[20,22]. Later, Yaqoob *et al.* reviewed the experimental information critically and reassessed the Ni-Mo system[33]. The number of parameters was reduced significantly compared with those of Zhou *et al.*[32]. However, the modeling of Yaqoob *et al.* can be further improved considering the following issues: (1) the enthalpy of mixing of the liquid phase is not in agreement with the experimental data[18,19]; (2) the enthalpy of formation of the δ phase at high temperature is lower than the experimental data[20,21]; (3) for the fcc phase, the SQS calculated enthalpy, the experimental Gibbs energy of mixing and the C_P at high temperature cannot be reproduced and (4) the magnetic properties of the fcc phase were ignored.

Mo-Re

Thermodynamic assessments of the Mo-Re system have been published by many authors[50–53]. Mathieu *et al.* reviewed all the previous work and performed reassessments aided by first-principles calculations[53]. A full five-sublattice (5SL) model and various simplified sublattice models of the σ phase were considered. Compared with the previous assessments, the thermodynamic properties calculated by Mathieu *et al.* show better agreement with the first-principles calculation data[53]. However, the homogeneity range of the σ phase at 1473 K calculated by Mathieu *et al.* (as well as other previous assessments) was very narrow. This is in contrast

Table 1. Performance accuracy (%) with patch images

Type of data		Reference	Method	Quoted mode[a]
Ni-Mo binary system				
Phase equilibria	70-85 at.% Ni	Grube *et al.* [7]		▮
	60-76 at.% Ni	Bloom *et al.* [8]		•
	fcc	Guthrie *et al.* [9]		○
	Overall	Casselton *et al.* [10]	TA, OM, XRD	○
	bcc liquidus	Wicker *et al.* [11]	CA, DTA	•
	Below 1600 K	Heijwegen *et al.* [12]	DC, EPMA	•
	fcc	Gust *et al.* [13]	(Not available)	•
	bcc solidus	Kang *et al.* [14]	EPS, EPMA	•
	fcc + Ni4Mo	Kobayashi *et al.* [15]	XRD	•
	bcc solidus, fcc + δ	Yaqoob *et al.* [3]	EA, EPMA	•
	1173K and 1073K	Zhu *et al.* [16]	DM, EPMA	•
	1373K and 1123K	Shi *et al.* [17]	DC, EA, SEM, XRD	•
Thermodynamic properties	Enthalpy of mixing of liquid	Chistyakov *et al.* [18]	Calorimetry	•
		Sudavtsova [19]	Calorimetry	▮
	Enthalpy of formation for δ, heat capacity for δ	Spencer *et al.* [20]	AC	•
	Enthalpies of formation for δ	Kubaschewski *et al.* [21]	AC	•
	Heat capacity of Ni_4Mo	Norem [22]	AC	•
		Brook *et al.* [23]	AC	▮
		Basak [24]	AC	▮
	Activity	Katayama *et al.* [25]	EMF	▮
		Meshkov *et al.* [26]	EMF	•
		Tsai *et al.* [27]	EMF	•
		Pejryd [28,29]	EMF	▮
		Koyama *et al.* [30]	EMF	•
		Sudavtsova [19]	EMF	▮
	Curie temperature	Khan *et al.* [34]	VSM, SQUID	•
	Magnetic moment	Ghosh *et al.* [35]	VSM, SQUID	•
Mo-Re system				
Phase equilibria	Overall	Dickinson *et al.* [36]	OM, XRD	•
		Knapton *et al.* [37]	OM, XRD	•
		Savitskii *et al.* [38,39]	OM, XRD	•
Thermodynamic properties	1473K and 1873K, enthalpy of formation	Farzadfar *et al.* [40]	OM, XRD, DRC	•
Ni-Mo-Re system				
Phase equilibria	1425K	Kodentsov *et al.* [41]	DC	▮
	1425K	Borisov *et al.* [42] Slyusarenko *et al.* [43]	DC & EA	•
	1473K	Feng *et al.* [44]	DM	▮
	1473K and 1873K, liquidus projection	Yaqoob *et al.* [3]	EA, EPMA, XRD	•
Thermodynamic properties	Site occupancy of σ	Yaqoob *et al.* [45]	XRD	•
	Heat capacity of NMR-75	Chekhovskoi *et al.* [45]	AC	▮

TA: Thermal analysis; OM: optical metallography; XRD: X-ray diffraction; CA: chemical analysis; DTA: differential thermal analysis; DC: diffusion couple; EPMA: electron probe microanalysis; EPS: electrolytic phase separation; EA: equilibrated alloys; DM: diffusion multiple; AC: adiabatic calorimetry; EMF: electromotive force; FP: first-principles calculations; VSM: vibrating sample magnetometer; SQUID: superconducting quantum interference device. aIndicates whether the data are used or not in the assessment: • used; ○: used partially; ▮: not used.

to the experimental data for not only the binary but also the ternary system. One may argue the accuracy of the experiments but it deserves a detailed study as discussed below. Moreover, when extrapolating the Mo-Re system with the parameters of Mathieu *et al.* to the ternary system[53], the Mo content in the bcc phase of the three-phase equilibria (i.e., bcc + δ + Mo_3CoSi and bcc + Mo_3CoSi + σ) was significantly higher than the experimental data, which is caused by a large value of $^1L_{Mo,Re}^{bcc}$ used to fit the equilibria between the bcc and σ phases.

Ni-Re

The experimental information of the Ni-Re binary system before 1985 has been reviewed critically by Nash *et al.* and an assessed Ni-Re phase diagram was reported[54]. Later, Yaqoob and Joubert reinvestigated experimentally and reassessed this binary system, and agreed well with most experimental data[6]. Furthermore, the invariant reaction temperature and corresponding compositions determined by Yaqoob and Joubert[6] were reconfirmed by Boettinger *et al.* [55]. Thus, the thermodynamic parameters from Yaqoob and Joubert[6] were

directly employed in the present work.

Ni-Mo-Re

Several experimental investigations have been carried out on the phase equilibria of the Ni-Mo-Re system [3,42,42−44]. Their measured phase diagrams are quite different in terms of the number and homogeneity ranges of the ternary intermetallic compounds.

The experimental data mainly considered in the present work are the phase equilibria of the Ni-Mo-Re system at 1473 and 1873 K determined by Yaqoob and Joubert [3] utilizing EPMA and XRD. The equilibrium annealing treatments for the alloys were at 1873 K for 9 h and at 1473 K for 70 d. The crystal structure identification of the ternary intermetallic compounds was carried out and two unknown ternary compounds were observed. One phase has a body-centered tetragonal crystal structure with a structure prototype Mo_3CoSi (named as bct in the present work) and the other has a modulated σ structure. The isothermal section measured by Yaqoob and Joubert [3] showed a large extension of the σ and δ phases and a limited extension of the x phase. The long annealing time and phase identification technique ensured the reliability of their work so that their result was used in the present work.

The phase equilibria at 1425 K were determined by Borisov *et al.* and Slyusarenko *et al.* using equilibrated alloys. The annealing time for the samples was 33.3 d [42,43]. The obtained isothermal section shows good compatibility with the work of Yaqoob and Joubert [3], except that only one ternary intermetallic compound was found. Borisov *et al.* and Slyusarenko *et al.* probably misinterpreted two phases as one single phase without performing phase identification [42,43]. Generally, these experimental data are considered reliable data.

The isothermal sections proposed by Kodentsov *et al.* and Feng *et al.* show poor agreement with that from Yaqoob and Joubert [3] and are therefore not utilized in the present assessment [41,44].

The site occupancies of the Ni-Mo-Re σ phase were determined by Yaqoob *et al.* as a function of composition in the ternary homogeneity domain, which were considered in the present work [45].

Chekhovskoi *et al.* measured the CP of the NMR-75 alloy (75 wt.% Ni, 15 wt.% Mo and 10 wt.% Re) in a temperature range of 300-1300 K. However, the results were not used in the present work since it was difficult to reproduce if other data were to be considered simultaneously [45].

FIRST-PRINCIPLES CALCULATIONS

First-principles calculations were performed using the Vienna ab initio simulation package (VASP) with plane-wave basis sets [56] based on density functional theory (DFT) [57]. Projector augmented wave pseudopotentials [58] were adopted to represent the valence electrons. GGA-PW91 [59] was adopted to describe the exchange and correlation effects. A large plane-wave cutoff energy of 400 eV was set for the plane-wave basis. The Monkhorst-Pack scheme [60] was used to construct the k-point meshes for Brillouin zone sampling. The spin-polarized calculations were performed with ferromagnetism set. The convergence criteria for electronic self-consistency and ionic minimization were 10^{-5} and 10^{-4} eV/unit cell, respectively. After relaxation, a final static calculation was conducted by employing the tetrahedron method with Blöchl corrections [61].

For the bcc, fcc and hcp solid solutions, the SQS method [62,63] was adopted to generate disordered structures for the VASP calculations. Supercells containing 16 atoms were constructed considering the configurations A12B4 and A15B1, where "A" denotes Ni for fcc, Mo for bcc and Re for hcp. Note that possible unstable structures, such as fcc Mo15Ni1, were not calculated since the full relaxation may not maintain the original structures. The total number of k-points multiplied by the total number of atoms per unit cell was at least 7200 for fcc, 6336 for bcc and 8000 for hcp. Using VASP, the SQS supercells were first relaxed with respect to

Table 2. Crystallographic and model information of stable phases in Ni-Mo-Re system

Phase	Pearson symbol	Prototype	Model
Liquid	-	-	$(Ni,Mo,Re)_1$
fcc_A1	cF4	Cu	$(Ni,Mo,Re)_1(VA)_1$
bcc_A2	cI2	W	$(Ni,Mo,Re)_1(VA)_3$
hcp_A3	hP2	Mg	$(Ni,Mo,Re)_1(VA)_{0.5}$
δ	oP56	NiMo	$(Ni)_{24}(Ni,Mo,Re)_{20}(Mo)_{12}$
Ni_3Mo	oP8	Cu_3Ti	$(Ni,Mo)_3(Ni,Mo)_1$
Ni_4Mo	tI10	Ni_4Mo	$(Ni)_4(Mo)_1$
σ	tP30	CrFe	$(Ni,Mo,Re)_2(Ni,Mo,Re)_4(Ni,Mo,Re)_8$ $(Ni,Mo,Re)_8(Ni,Mo,Re)_8$
x	cI58	α-Mn	$(Ni,Mo,Re)_2(Ni,Mo,Re)_8(Ni,Mo,Re)_{24}$ $(Ni,Mo,Re)_{24}$
bct	tI56	Mo_3CoSi	$(Mo,Re)_9(Ni,Re)_4(Ni)_1$

cell volume only, then to volume and cell shape, and finally simultaneously to volume, cell shape and atomic position (i.e., full relaxation) in the present work. On this basis, a fast convergence speed can be achieved. To check the symmetry preservation, the radial distribution functions were analyzed[64].

In addition, VASP calculations were also performed to obtain the formation energies of all the end-members of the σ and x phases. The k-point meshes were $12 \times 12 \times 12$ and $8 \times 8 \times 15$, respectively. To facilitate the calculations, the ZenGen script-tool[65] was adopted to conveniently generate input files for the VASP calculations.

THERMODYNAMIC MODELS

In the Ni-Mo-Re system, the stable phases included in this assessment are liquid, fcc, bcc, hcp, δ, Ni_3Mo, Ni_4Mo, σ, x and the bct phase with a Mo_3CoSi structural prototype. Their crystal structure information and the thermodynamic models are summarized in Table 2. The thermodynamic descriptions of the pure elements Ni, Mo and Re were taken from the Scientific Group Thermodata Europe (SGTE) unary database (Version 5.0)[66]. All the phases were described by the sublattice model within CEF. Detailed mathematical expressions are available in our previous work[67].

Solution phases

The solution phases (including liquid, fcc, bcc and hcp) were treated as substitutional solutions and described by a substitutional solution model with the Redlich-Kister polynomials[68].

Normally, for the interaction parameter, a linear temperature dependence is sufficient, i.e., $^nL_{i,j}^{\varphi} +^n a_{i,j} +^n b_{i,j}T$. In the present work, the measured excess heat capacity for the fcc phase of the Ni-Mo system is available, so a $Tln(T)$ term was introduced to produce a constant excess heat capacity.

Intermetallic phases

In the present work, three intermetallic phases, i.e., δ, Ni_3Mo and Ni_4Mo, were considered for the Ni-Mo system. The solubility of Re was ignored in both Ni_3Mo and Ni_4Mo due to the lack of experimental data.

The molar Gibbs energy of each intermetallic phase φ is described as:

$$G_m^{\varphi} = \sum_I y_i^s {}^oG_I^{\varphi} + RT\left(\sum_s a^s \sum_i y_i^s \ln y_i^s\right) + {}^{ex}G_m^{\varphi}; \tag{1}$$

where y_i^s is the site fraction of component i in the sublattice s, $^oG_I^{\varphi}$ is the Gibbs free energy of the end member I, R is the gas constant, a^s as is the number of sites of sublattice s and $^{ex}G_m^{\varphi}$ corresponds to the molar excess

Gibbs energy, expressed in the Redlich-Kister polynomial.

Although the Ni_3Mo compound with the $D0_a$ structure is stoichiometric in the Ni-Mo system, the phase with the same structure is non-stoichiometric in some ternary systems, such as Ni-Mo-Ta, modeled as $(Ni,Mo,Ta)_3(Ni,Mo,Ta)_1$ by Cui *et al.* [48]. To extend to high-order systems for a multi-component Ni-based database, the two-sublattice model of $(Ni,Mo)_3(Ni,Mo)_1$ was also adopted in the present work.

For non-stoichiometric phase Ni_3Mo, the Kopp-Neumann rule was applied to estimate the C_P of end-members based on the composition average of the C_P of the pure elements in their stable element reference (SER) at 298 K, i.e., fcc Ni, bcc Mo and hcp Re. Its Gibbs energy per mole of the formula of the end-members can be expressed as:

$$^oG_{i:j}^{Ni,Mo} = 3{}^oG_i^{SER} + {}^oG_j^{SER} + a + bT \qquad (2)$$

Following the previous assessment for the Ni-Mo binary, the δ phase was modeled as $(Ni)_{24}(Ni,Mo)_{20}(Mo)_{12}$, a simplified model of $(Ni)_{24}(Ni,Mo)_{20}(Mo)_8(Mo)_4$. The coordination numbers (CNs) of the three sublattices are 12, 14 and 15/16, respectively. Since the atomic size of Re is medium among the three elements, Yaqoob [2] assumed that Re only occupies the second sublattice (i.e., CN = 14), which was adopted in the present work. Therefore, the model for the δ phase was extended to $(Ni)_{24}(Ni,Mo,Re)_{20}(Mo)_{12}$.

The end-members of the δ phase can be described by Eq. (3), in which the parameter a was fixed to the enthalpy data from Zhou *et al.* (except that of the end-member Ni:Re:Mo, which was quoted from Yaqoob [2]) and b is the entropy term to be evaluated based on phase equilibria [32]. As the enthalpy data measured at high temperature are available, a $TlnT$ term may be needed as follows:

$$^oG_{i:j:k}^{\delta} = 24{}^oG_i^{SER} + 20{}^oG_j^{SER} + 12{}^oG_k^{SER} + a + bT + cT\ln T \qquad (3)$$

Because of the limited solubility range reported by Heijwegen and Rieck [12], Kobayashi *et al.* and Zhu *et al.*, the Ni_4Mo phase was treated as a stoichiometric compound [15,16]. Since C_P for the Ni_4Mo phase is known, the Gibbs energy per mole of formula Ni_4Mo is parameterized to fit the C_P data with a power series in temperature as follows:

$$G_m^{Ni_4Mo} = a + bT + cT\ln T + dT^2 \qquad (4)$$

where the parameters c and d were obtained from the C_P data and the parameters a and b were evaluated based on phase equilibria and enthalpy data.

There exist two intermetallic phases (i.e., σ and x) in the binary Mo-Re system. The σ phase is the most important phase in the Ni-Mo-Re system. Ideally, the σ phase should be modeled as a 5SL model. In contrast, the simplified three-sublattice model (3SL), i.e., $(Ni,Mo,Re)_{10}(Ni,Mo,Re)_4(Ni,Mo,Re)_{16}$ is also widely used to reduce the end-members. Figure 1 shows the calculated Gibbs energy of the σ phase at 298 K along 0.5Mo0.5Re-Ni and binary Mo-Re using the 5SL and 3SL models, respectively, with the formation enthalpies of all the end-members in Eq. (1) determined by VASP data calculated in the present work. Obviously, the 5SL model manifests two composition sets of the σ phase in the ternary system and theoretically predicts the composition sets, which is consistent with the experimental finding of Yaqoob *et al.* [6].

The simplified 3SL fails to capture this structural relationship using the VASP data (mainly representing nearest-neighbor interactions) only. One can use positive interaction parameters within a sublattice to produce the composition sets. However, since there are only 23 binary end-members in the 3SL model, no suitable interaction parameters can be used to adjust the composition sets according to the experimentally determined composition range. For a detailed explanation, see **Appendix I**.
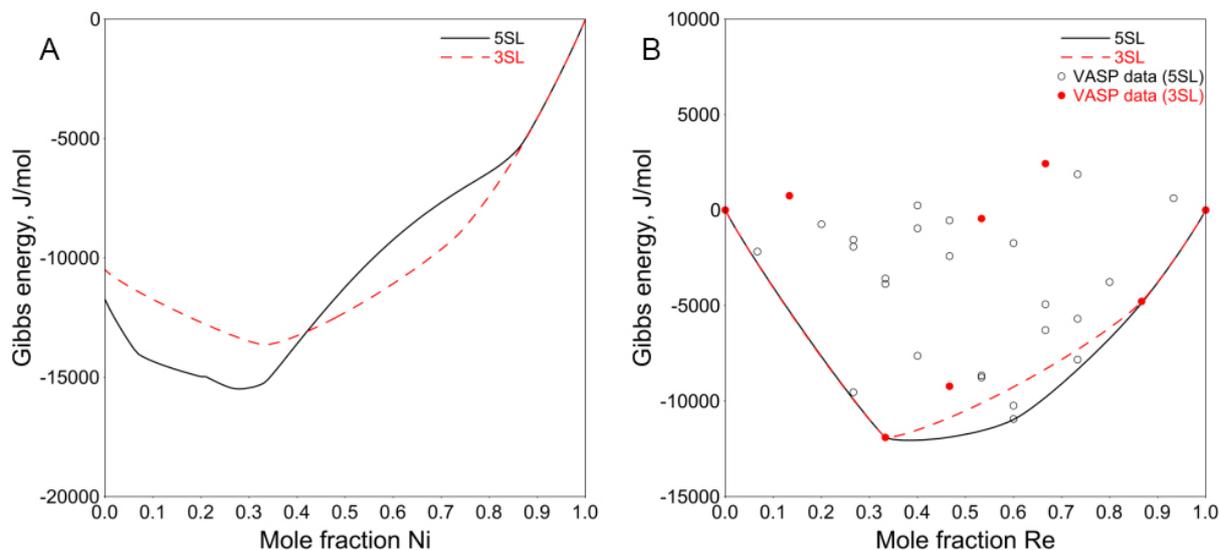
Figure 1. Calculated Gibbs energy of σ phase at 298 K along (A) 0.5Mo0.5Re-Ni and (B) Mo-Re using the 5SL and 3SL models compared with the VASP results. Sigma Ni, sigma Mo and sigma Re are used as reference states.

Therefore, the 5SL model combined with the VASP data was adopted in the present work to ensure reasonable modeling of the σ phase and its modulated counterpart.

The Gibbs energy of an end-member of σ is expressed as follows:

$$^{o}G^{\sigma}_{ABCDE} = \sum_{s} a^{s \, o} G^{SER}_{i} + E^{\sigma}_{ABCDE} - \sum_{s} a^{s} E^{SER}_{i} - T \left(S^{\sigma}_{ABCDE} - \sum_{s} a^{s} S^{SER}_{i} \right) \qquad (5)$$

where G^{σ}_{ABCDE} is the Gibbs free energy of the end-member ABCDE, E^{σ}_{ABCDE} and E^{SER}_{i} are the DFT energies of $ABCDE$ in the σ structure and that of element i in its SER structure, respectively, and S^{σ}_{ABCDE} and S^{SER}_{i} are the entropies of $ABCDE$ in the σ structure and that of element i in its SER structure, respectively. Mathieu *et al.* simplified the equation when studying the σ phase of the Mo-Re system [53]. They approximated S^{σ}_{ABCDE} as $\sum_{s} a^{s} S^{\sigma}_{i}$, where is the entropy of element i in the σ structure. On this basis, the entropy difference $\Delta S^{\sigma-SER}_{i} = S^{\sigma}_{i} - S^{SER}_{i}$ is introduced and the Gibbs free energy of the end-member $ABCDE$ is thus expressed as:

$$^{o}G^{\sigma}_{ABCDE} = \sum_{s} a^{s \, o} G^{SER}_{i} + E^{\sigma}_{ABCDE} - \sum_{s} a^{s} E^{SER}_{i} - T \sum_{s} a^{s} \Delta S^{\sigma-SER}_{i} \qquad (6)$$

This simplification reduces the number of model parameters remarkably. It is necessary because it is difficult to determine the entropy of $ABCDE$ in the σ structure.

For σ, the molar excess Gibbs energy $^{ex}G^{\sigma}_{m}$ in Eq. (1) is used to describe the interactions within a sublattice [53].

The x phase has a bcc crystal structure, in which 58 atoms are distributed over four sublattices. A four-sublattice model of $(Ni,Mo,Re)_2(Ni,Mo,Re)_8(Ni,Mo,Re)_{24}(Ni,Mo,Re)_{24}$ was used and its Gibbs free energy is similar to that of σ.

The unit cell of the bct phase contains 56 atoms distributed over six sites with CNs of 10, 12, 14 and 15. The sites with low CNs of 10 and 12 are shared by small and intermediate size atoms (Si and Co, respectively), the site

with a CN of 14 is occupied by intermediate and large atoms (Co and Mo, respectively) and the site with a CN of 15 contains large atoms (Mo). Based on the observed XRD pattern and EPMA-determined composition of the phase, Yaqoob[2] removed the intermediate size Re from the site with a CN of 10 and placed it on the site with a CN of 15 along with Mo. Therefore, the bct phase was described using a 3SL model of $(Mo,Re)_9(Ni,Re)_4(Ni)_1$. The first sublattice combines the sites with CNs of 14 and 15, the second sublattice groups the sites with a CN of 12 and the third is the site with a CN of 10.

The Gibbs free energy of bct is expressed by Eq. (1) and one of its end-members I is described by:

$$^oG_I^{bct} = \sum_s a^s \, ^oG_i^{SER} + a + bT \tag{7}$$

where the parameter a was fixed to the DFT data calculated by Yaqoob[2]. The parameter b, corresponding to the entropy of formation of the end-members, was assessed together with the excess Gibbs energy based on phase equilibrium data.

RESULTS AND DISCUSSION

For solution phases, in the first step, the a terms for the interaction parameters were assessed using the SQS and measured enthalpy. In the second step, the b terms representing the influence of temperature on the interaction parameters were assessed based on the phase diagram and activity data.

For intermetallics, the enthalpy terms for the end-members were fixed to the VASP calculated data, while the entropy terms of the end-members were assessed based on the phase diagram data. As a final step, all parameters may be adjusted slightly to fit the experimental data better.

The thermodynamic parameters for phases in the present work are listed in **Appendix II**. A full database for the Ni-Mo-Re ternary system is provided in the supplementary material.

Ni-Mo system

In general, the assessment of Zhou *et al.* is not as satisfactory as that of Yaqoob *et al.*[32,33]. Therefore, only the results of Yaqoob *et al.* are compared with the present work in the following discussion. Figure 2 shows the calculated phase diagram compared with experimental data[8–17], as well as the previous assessment[33]. The experimental data that were not mentioned by Yaqoob *et al.* are colored. It is difficult to fit the homogeneity domain of the δ phase and the fcc solvus in equilibrium with the Ni_4Mo phase at low temperatures. The results of Zhou *et al.* show good agreement for these phase equilibria but the cost is the poor agreement with the measured C_P of the Ni_4Mo phase[32]. The present assessed phase diagram is similar to that of Yaqoob *et al.*, except for the homogeneity range of the δ phase and the related invariant reaction temperature[33]. However, the main improvements of the present work were on the thermodynamic properties, as discussed below.

Figure 3A shows the enthalpy of mixing for the liquid phase. Chistyakov *et al.* and Sudavtsova measured the enthalpy of mixing of liquid using calorimetry at 1823 and 1874 K, respectively[18,19]. The experimental results from Sudavtsova are lower than those from Chistyakov *et al.*[18,19]. It is difficult to estimate which one is better. In the present assessment, Sudavtsova's results were found to be too negative that the bcc liquidus would be higher than the experimental data when the temperatures for invariant reactions were fixed. Moreover, considering that the experimental procedure of Chistyakov *et al.* was more detailedly described than that by Sudavtsova, the results from Chistyakov *et al.* were adopted in the present work[18].

Figure 3B shows the assessed enthalpies of mixing for solution phases at 298 K compared with the SQS data[32,33]. As noted above, the SQS calculations were performed only for stable structures in the present
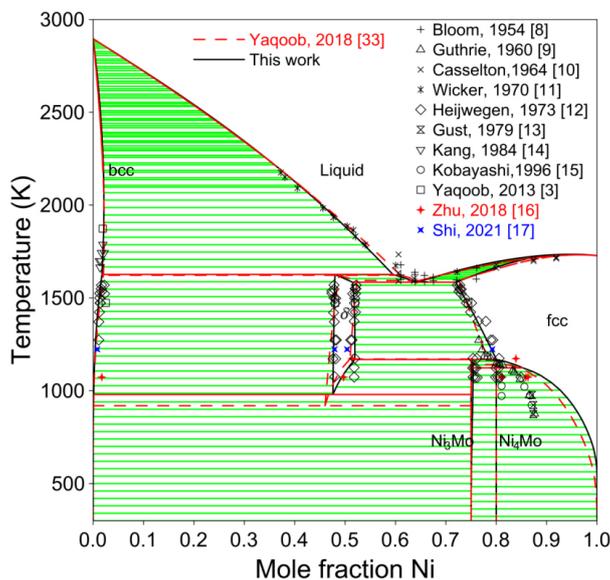
Figure 2. Comparison of calculated Ni-Mo phase diagram with experimental data.
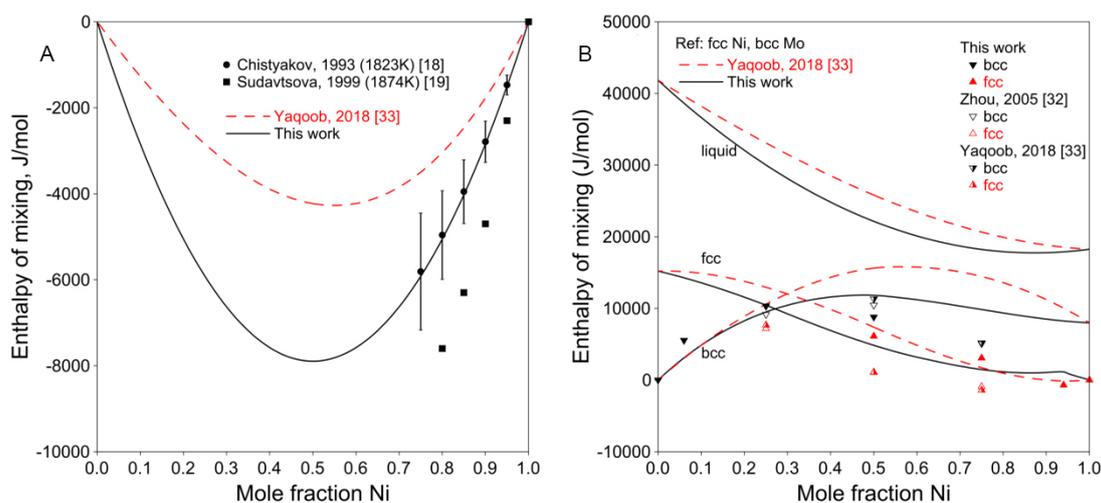
Figure 3. (A) Assessed enthalpy of mixing for liquid at 1873 K compared with experimental data. (B) Assessed enthalpy of mixing for solution phases at 298 K compared with SQS results for Ni-Mo system.

work, since possible unstable structures, such as fcc Mo or bcc Ni, may not be maintained during the full relaxation. Therefore, the SQS enthalpies of mixing from Zhou *et al.* and Yaqoob *et al.* were not used in the assessment[32,33]. Figure 3B shows a positive enthalpy for the bcc phase, indicating instability at low temperatures, which is in accordance with the phase diagram shown in Figure 2, where there is less than 3.0 at.% Ni soluble in bcc Mo at low temperatures.

Figure 4A shows the assessed formation enthalpies of Ni_4Mo and Ni_3Mo compared with the DFT data and previous assessments. Compared to earlier thermodynamic assessments[47,48], the assessed enthalpies of formation in the present work are more reliable with the help of DFT calculation. There are experimental data in Figure 4B showing that the C_P of fcc does not follow the Kopp-Neumann rule (red dashed line for fcc), so an extra term $CTln(T)$ was used in order to fit the experimental data. The data measured by Brooks and Meschter[23] deviate largely from the assessment but agree well with the calculated C_P at 78 at.% Ni (dotted
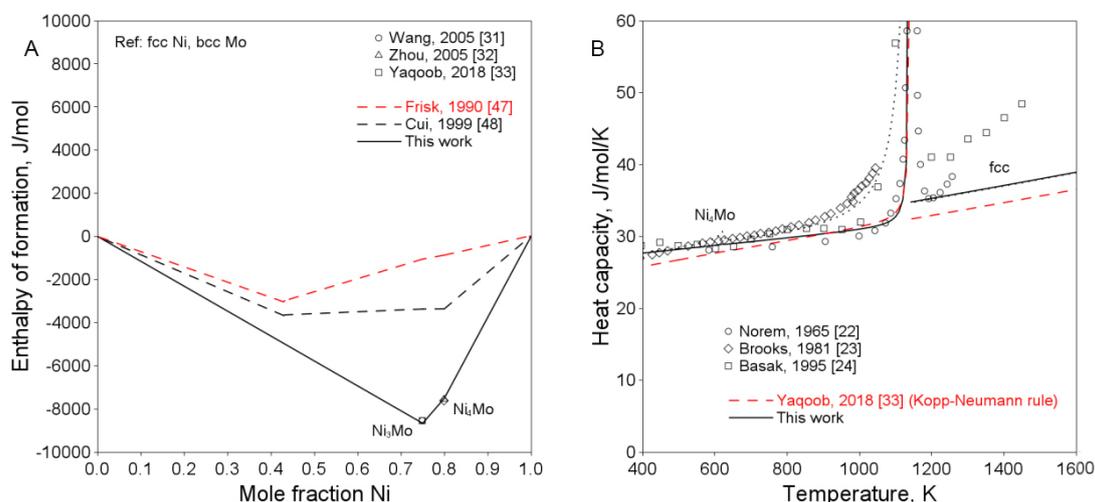
Figure 4. (A) Assessed enthalpy of formation at 298 K compared with DFT data. (B) Assessed heat capacities of Ni_4Mo and fcc at 80 at.% Ni compared with experimental data (dotted line represents the calculated C_P at 78 at.% Ni).

line). There was probably a deviation in the composition of the sample in the experiments by Brooks and Meschter.

Mo-Re system

Knapton[37] conducted a careful study of this system by means of melting-point measurements, XRD and metallographic methods, using both powder-metallurgical and arc-melting samples. Knapton did not clarify which preparation method was used for each piece of data clearly. However, he showed that between 1673 and 1873 K, only the σ phase was stable at ~68 at.% Re, while in the immediate vicinity of 70 at.% Re, the σ phase decomposed. This means that the single σ phase region can reach as far as 68 at.% Re between 1673 and 1873 K. All other available experimental data[3,36,38–40] also manifest a wide single σ phase region over a wide temperature range in the binary Mo-Re system. In addition, the previously assessed homogeneity range of the σ phase at low temperatures was so narrow that the extrapolation to the ternary system cannot agree with the experimental data[3], which will be discussed in the following ternary assessment. Any attempt to reproduce a U-shape σ phase boundary led to a very poor fit of site occupancy. Considering the wide single σ phase region over a wide temperature range and the fact of difficulty reaching equilibrium at lower temperatures, the estimated eutectoid temperature may need further confirmation.

As mentioned in the literature review, when extrapolating the Mo-Re system with the parameters of Mathieu *et al.* to the ternary system, the bcc phase of the three-phase equilibria (i.e., bcc + δ + bct and bcc + bct + σ) has a relatively high Mo content comparing to the experimental data[3,53]. It was found that the Gibbs energy of the binary bcc phase assessed by Mathieu *et al.* was too positive by giving the sub-regular solution parameter (i.e., $^1L_{Mo,Re}^{bcc}$) in order to reduce the binary bcc+σ two-phase region[53]. Thus, in the present work, a regular solution model was adopted to solve the problem.

Figure 5 shows the present calculated phase diagram of the Mo-Re system and the assessment by Mathieu *et al.* together with the experimental data[3,36–40,53]. A larger σ phase region is realized but fails at the Re-rich side as the site occupancy discussed below exerts a constraint. Furthermore, the bcc single phase at 2673 K and ~40 at.% Re was not fitted by Mathieu *et al.* but is well considered in the present work[53].

Figure 6 shows the calculated enthalpies of mixing at 298 K together with the SQS data from Mathieu *et al.*[53].
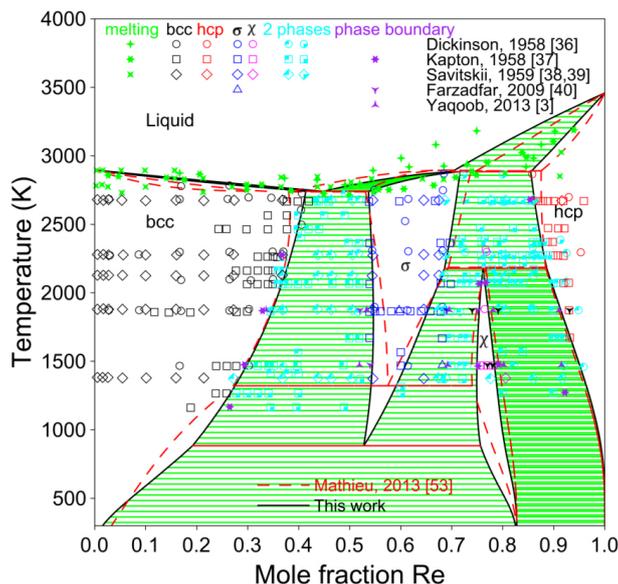
Figure 5. Assessed Mo-Re phase diagram compared with experimental data and assessment by Mathieu *et al.*[53].
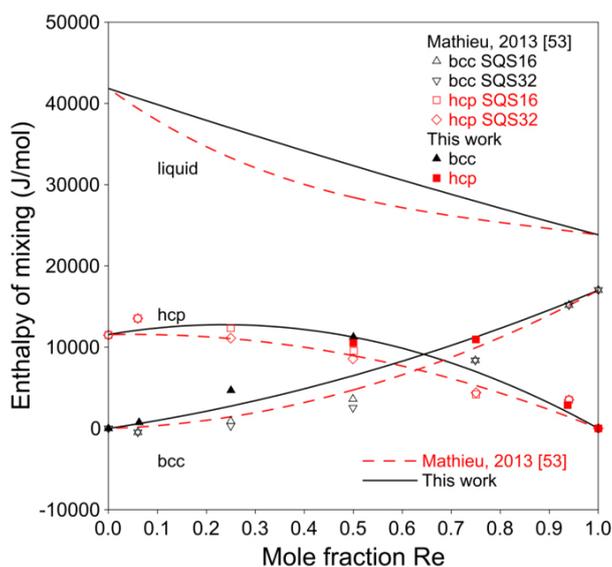
Figure 6. Assessed enthalpy of mixing of Mo-Re bcc and hcp phases compared with SQS data.

The present model can well predict the site fractions, as shown in Figure 7. Mathieu *et al.* did not use excess energy terms for the σ and x phases because they assumed that all the interactions characterizing the phase were taken into account by the DFT calculations[53]. For the σ phase, the VASP data can predict the site fractions perfectly without any interaction parameter. However, it is necessary to introduce interaction parameters for the x phase to fit the site fractions of the 2A and 8C sites.

Ni-Mo-Re system

Isothermal sections

Figure 10 compares the assessed isothermal sections at 1425, 1473 and 1873 K with the experimental data. Since the Ni-Mo-Re system was assessed mainly based on the experimental data by Yaqoob *et al.*, it is impossible to reproduce the phase equilibria concerning the σ phase measured by Borisov *et al.* at 1425 K[3,42]. For other
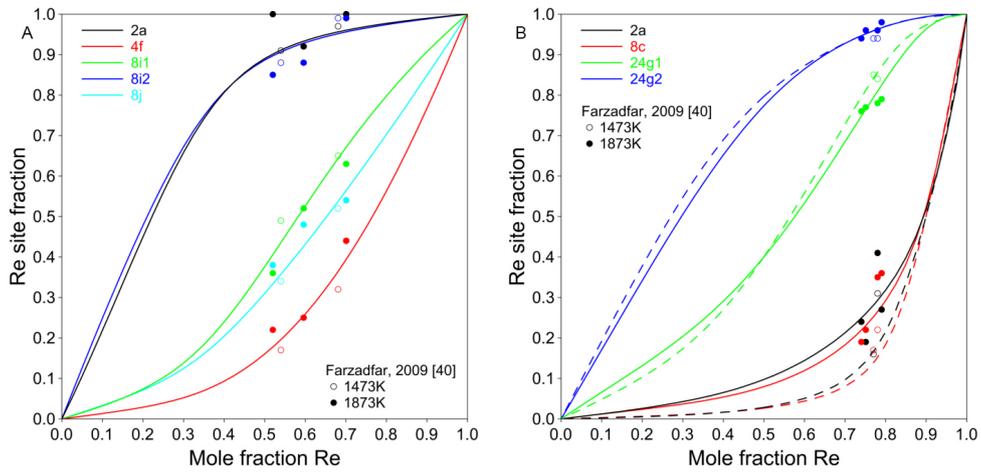
Figure 7. Calculated site fractions of Re for (A) Mo-Re σ and (B) x at 1673 K. In (B), the solid lines represent the case considering the interaction parameter L, while dashed lines represent the case without L.
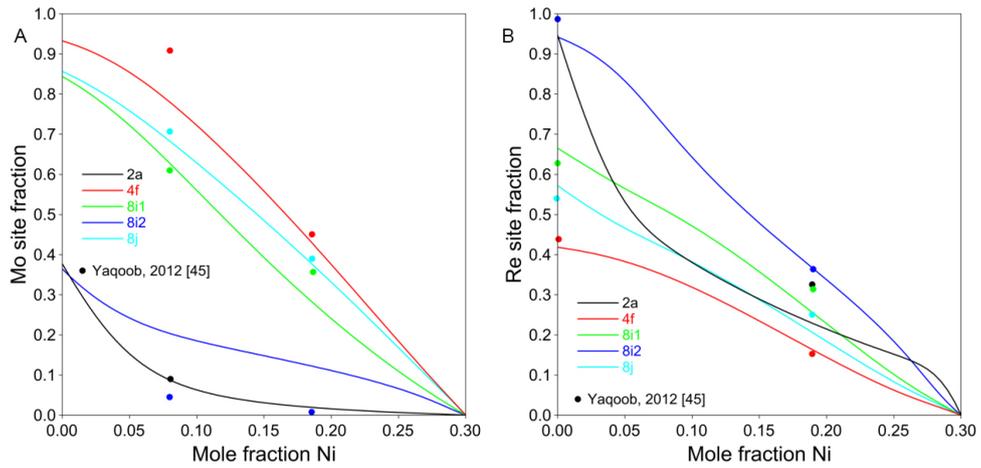
Figure 8. Calculated site fractions for Ni-Mo-Re σ phase at 1873 K for (A) Mo along $Mo_{0.7}Re_{0.3}$-$Ni_{0.3}Re_{0.7}$ and (B) Re along $Mo_{0.3}Re_{0.7}$-$Ni_{0.3}Mo_{0.7}$.
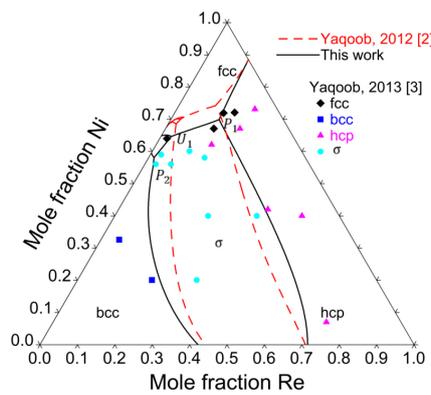
Figure 9. Assessed primary crystallization surface of Ni-Mo-Re ternary system compared with experimental data.

phase equilibria, there is no conflict between the results reported by Borisov *et al.* and Yaqoob *et al.*[3,42]. The
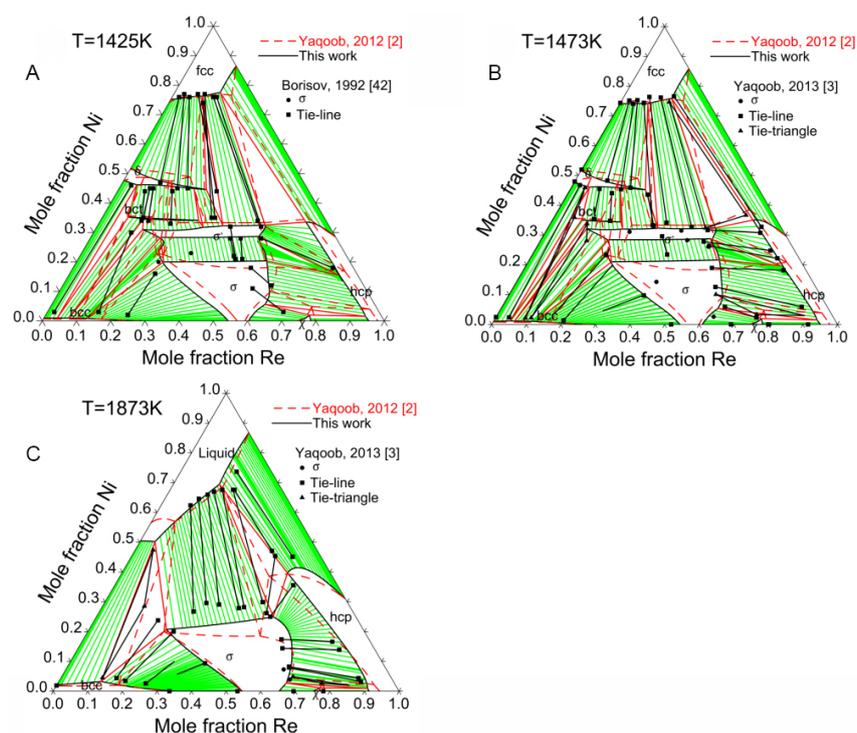
Figure 10. Calculated isothermal sections of Ni-Mo-Re ternary system at (A) 1425, (B) 1473 and (C) 1873 together with experimental data.

calculated isothermal sections present a good agreement with the experimental data, especially the extended σ single-phase region in the ternary system. The two composition sets for the σ phase are well reproduced.

By applying the 5SL model, the site fractions and the ordering behavior of the ternary σ phase can also be examined as a function of composition and temperature. In Figure 8, the calculated site fractions are in reasonable agreement with the experimental data at 1873 K.

Primary crystallization surface
The primary crystallization surface was assessed using the experimental data from Yaqoob *et al.* and presented in Figure 9, where there are five primary crystallization surfaces, namely, fcc, bcc, hcp, δ and σ [3]. It is difficult to perfectly fit the primary surfaces of the hcp and fcc phases since their thermodynamic parameters were primarily determined according to the isothermal sections at 1473 and 1873 K.

CONCLUSIONS

The present work adopts the CALPHAD method to analyze a large amount of experimental and DFT data concerning the thermodynamics and phase diagrams of the Ni-Mo-Re alloy system. It demonstrates that the CALPHAD method can act as a practical appliance in the toolbox of materials informatics to assess various data by consistent modeling and then produce more useful data by computational predictions.

The Ni-Mo and Mo-Re binary systems were reassessed to obtain a better agreement with the experimental data. The large homogeneity range of the σ phase in the Mo-Re system was examined and considered. For the Ni-Mo-Re ternary system, the reliability of the present model parameters was confirmed by the comprehensive comparison between the assessed and experimental data, i.e., three isothermal sections, site occupancy and primary crystallization surface. In particular, the 5SL modeling of the σ phase enables a satisfactory description of the co-existence of the σ phase and its modulated variant σ' structure.
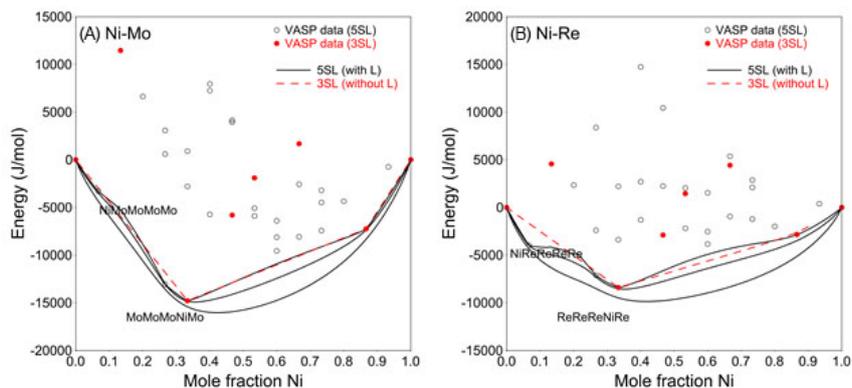
Appendix I

By using the 5SL model for the sigma phase, positive values of the binary parameters $^0L^\sigma_{*:*:*:Ni,Mo:*}$ and $^0L^\sigma_{*:*:*:Ni,Re:*}$ ncrease the enthalpies between the end-members NiMoMoMoMo and MoMoMoNiMo for Ni-Mo, NiReReReRe and ReReReNiRe for Ni-Re, respectively. These parameters lead to two composition sets at the low Ni region in the Ni-Mo and Ni-Re binary systems (see the following two figures: left for Ni-Mo, right for Ni-Re).

However, these end-members in the binary systems (such as NiMoMoMoMo and MoMoMoNiMo, see figures below) do not exist when using 3SL, so no interaction parameters can be used to adjust the MG. In conclusion, 3SL cannot reproduce the experimentally determined MG.

Appendix II

Thermodynamic parameters of the Ni-Mo-Re system assessed in the present work

Liquid

$^0L^{Liquid}_{Ni,Mo}$=-31580+9.1T

$^0L^{Liquid}_{Mo,Re}$=-2000

$^0L^{Liquid}_{Ni,Mo,Re}$=0

$^1L^{Liquid}_{Ni,Mo,Re}$=0

$^2L^{Liquid}_{Ni,Mo,Re}$=-30000

fcc

$^0L^{fcc}_{Ni,Mo}$=-17930+119.69T-15.1Tln T

$^1L^{fcc}_{Ni,Mo}$=12700

$\beta^{fcc}_{Ni,Mo}$=-3.5

$^1T^{fcc}_{CNi,Mo}$=-5500

$^0L^{fcc}_{Ni,Mo,Re}$=87840-85T

$^1L^{fcc}_{Ni,Mo,Re}$=97840-80T

$^2L^{fcc}_{Ni,Mo,Re}$=0

bcc

$^0L^{bcc}_{Ni,Mo}$=27191

$^1L^{bcc}_{Ni,Mo}$=18792

$^0L^{bcc}_{Mo,Re}$=-8000+3.5T

$^0L^{bcc}_{Ni,Mo,Re}$=40380-20T

$^1L^{bcc}_{Ni,Mo,Re}$=0

$^2L^{bcc}_{Ni,Mo,Re}$=50000

hcp

$^0L^{hcp}_{Mo,Re}$=21850-5.2T

$$^0L^{hcp}_{Ni,Mo,Re}=243650-50T$$
$$^1L^{hcp}_{Ni,Mo,Re}=160950-150T$$
$$^2L^{hcp}_{Ni,Mo,Re}=-60000$$

δ

$$^0G^{\delta}_{Ni:Mo:Re}=24\,^0G^{fcc}_{Ni}+32\,^0G^{bcc}_{Mo}-238250+1397T-185T\ln(T)$$
$$^0G^{\delta}_{Ni:Ni:Mo}=44\,^0G^{fcc}_{Ni}+12\,^0G^{bcc}_{Mo}-74620+2340T-292T\ln(T)$$
$$^1G^{\delta}_{Ni:Ni:Mo:Mo}=-294600+450T$$
$$^0G^{\delta}_{Ni:Re:Mo}=24\,^0G^{fcc}_{Ni}+20\,^0G^{bcc}_{Mo}-12\,^0G^{hcp}_{Re}-329112$$
$$^0G^{\delta}_{Ni:Ni:Re:Mo}=302700$$

Ni$_3$Mo

$$^0G^{Ni_3Mo}_{Ni:Ni}=4\,^0G^{fcc}_{Ni}+11360+15T$$
$$^0G^{Ni_3Mo}_{Ni:Mo}=3\,^0G^{fcc}_{Ni}+\,^0G^{bcc}_{Mo}-40160+23.2T$$
$$^0G^{Ni_3Mo}_{Ni:Ni}=3\,^0G^{bcc}_{Mo}+\,^0G^{fcc}_{Ni}+68240$$
$$^0G^{Ni_3Mo}_{Mo:Mo}=4\,^0G^{bcc}_{Mo}+170600$$

Ni$_4$Mo

$$G^{Ni_4Mo}_m=-76820+734T-128T\ln(T)-0.013T^2$$

σ

$$\triangle S^{\sigma-SER}_{Ni}=2.4$$
$$\triangle S^{\sigma-SER}_{Mo}=-1.5$$
$$\triangle S^{\sigma-SER}_{Re}=-1.2$$
$$^0L^{\sigma}_{*:*:*:Ni,Mo:*}=20700$$
$$^0L^{\sigma}_{*:*:*:Ni,Re:*}=20700$$
$$^0L^{\sigma}_{*:*:*:Ni,Mo,Re:*}=-1050000$$

χ

$$\triangle S^{\chi-SER}_{Ni}=1.3$$
$$\triangle S^{\chi-SER}_{Mo}=-2.42$$
$$\triangle S^{\chi-SER}_{Re}=0.85$$
$$^0L^{\chi}_{Mo,Re:*:*:*}=-30T$$
$$^0L^{\chi}_{*:Mo,Re:*:*}=-100T$$
$$^0L^{\chi}_{*:*:Mo,Re:*}=-100T$$

bct

$$^0G^{bct}_{Mo:Ni:Ni}=9\,^0G^{bcc}_{Mo}+5\,^0G^{fcc}_{Ni}-22110-7T$$
$$^0G^{bct}_{Re:Ni:Ni}=9\,^0G^{hcp}_{Re}+5\,^0G^{fcc}_{Ni}-7812+20T$$
$$^0G^{bct}_{Mo:Re:Ni}=9\,^0G^{bcc}_{Mo}+4\,^0G^{hcp}_{Re}+\,^0G^{fcc}_{Ni}+69748$$
$$^0G^{bct}_{Re:Re:Ni}=13\,^0G^{hcp}_{Re}+\,^0G^{fcc}_{Ni}+153020$$
$$L^{bct}_{Mo,Re:*:Ni}=-120000$$

DECLARATIONS

Authors' contributions
Writing and editing: Lei XH, Lu XG
First-principles calculations: Liu W
Data analysis and discussion: Lei XH, Liu W, Luo F, Lu XG

Availability of data and materials
Supplementary materials are available from the Journal of Materials Informatics or from the authors.

Conflicts of interest
The authors declared that there are no conflicts of interest.

Ethical approval and consent to participate
Not applicable.

Consent for publication
Not applicable.

REFERENCES

1. Reed RC. The superalloys fundamental and applications, Cambridge University Press, New York, 2008. DOI
2. Yaqoob K. Thesis. Paris-Est Créteil University, 2012. Available from: https://www.theses.fr/2012PEST1172.pdf [Last accessed on 29 Jul 2022]
3. Yaqoob K, Joubert J. Experimental investigation of the Mo-Ni-Re system. *J Alloys Compd* 2013;559:101-11. DOI
4. J.-C. Crivello. Unpublished work.
5. Yaqoob K, Guénée L, Černý R, Joubert J. A modulated structure derived from the σ phase in the Mo-Ni-Re system. *Intermetallics* 2013;37:42-5. DOI
6. Yaqoob K, Joubert J. Experimental determination and thermodynamic modeling of the Ni-Re binary system. *J Solid State Chem* 2012;196:320-5. DOI
7. Grube G, Vosskühler H. Elektrische Leitfähigkeit und Zustandsdiagramm bei binären Legierungen. 8. Mitteilung. Das System Lithium-Zink. *Z Anorg Allg Chem* 1933;215:211-24. DOI
8. Bloom DS, Grant NJ. An investigation of the systems formed by chromium, molybdenum, and nickel. *JOM* 1954;6:261-8. DOI
9. P.V. Guthrie, E.E. Stansbury, X-ray and metallographic study of the nickel-rich alloys of the nickel-molybdenum system. II, Oak Ridge National Laboratory, Oak Ridge, Tennessee, 1961, p. 57. DOI
10. Casselton R, Hume-rothery W. The equilibrium diagram of the system molybdenum-nickel. *J Less Comm Metals* 1964;7:212-21. DOI
11. A. Wicker, C. Allibert, J. Driole, E. Bonnier, Etude d' équilibres de phases dans les systèmes Ni-Nb-Mo, Ni-Nb et Ni-Mo, Comptes Rendus l'Acad. Sci. Sér. C 271 (1970) 273-275. DOI
12. Heijwegen CP, Rieck GD. Determination of the phase diagram of the molybdenum-nickel system using diffusion couples and equilibrated alloys. *Inter J Mater Res* 1973;64:450-3. DOI
13. W. Gust, T. Nguyen-Tat, B. Predel, untersuchungen zur dikontinuierlichen ausscheidung in einer Ni-Mo-Legierung mit 17.5 at.% Mo, Z. Metallkd. 70 (1979) 241-246. DOI
14. Kang SL, Song Y, Kaysser WA, Hofmann H. Determination of Mo solidus in the Mo-Ni system by electrolytic phase separation method. *Inter J Mater Res* 1984;75:86-91. DOI
15. Kobayashi S, Sumi T, Koyama T, Miyazaki T. Determination of coherent phase boundaries in Ni-V and Ni-Mo alloys by utilizing macro-scopic composition gradient. *J Japan Inst Metals* 1996;60:22-8. DOI
16. Zhu L, Wei C, Jiang L, Jin Z, Zhao J. Experimental determination of the phase diagrams of the Co-Ni-X (X = W, Mo, Nb, Ta) ternary systems using diffusion multiples. *Intermetallics* 2018;93:20-9. DOI
17. Shi J, Guo C, Li C, Du Z. Experimental investigation of intermetallics and phase equilibria in the Hf-Mo-Ni system at 1100 °C and 950 °C. *Metall Mater Trans A* 2021;52:1059-76. DOI
18. ChistyakovLS , Grigorovich KV, Stomakhin AY. Enthalpy of formation of liquid Ni-Mo alloys, Izv. Vyss. Uchebn. Zaved. Chern. Metall. (1993) 82-83. DOI
19. Sudavtsova VS. Thermodynamic properties of melts of Ni-Cr(Mo,W) binary systems, Russ. Metall. 1999;118-120. DOI
20. Spencer P, Putland F. A calorimetric study of intermediate phases in iron +, cobalt +, and nickel + molybdenum. *J Chem Thermodyn* 1975;7:531-6. DOI
21. Kubaschewski O, Hoster T. Bildungs- und Umwandlungs-Enthalpien in binären und ternären Systemen der Metalle Eisen, Kobalt, Nickel und Molybdän. *International J Mater Res* 1983;74:607-9. DOI
22. Norem, WE, Ph.D. Thesis. University of Tennessee, Knoxville, 1965.
23. Brooks CR, Meschter PJ. A Combined Thermodynamic Study of Nickel-Base Alloys, Department of Energy, Knoxville, Tennessee, 1981, p. 42. DOI
24. Basak D. Application of Pulse Calorimetry to Metal Systems, (n.d.) 248. DOI

25. Katayama I, Shimatani H, Kozuka Z. Thermodynamic study of solid Cu-Ni and Ni-Mo alloys by E.M.F. Measurements using the solid electrolyte. *J Japan Inst Metals* 1973;37:509-15. DOI

26. Meshkov LL, Guzei LS, Sokolovskaya EM. Sokolovskaia, thermodynamics of nickel-molybdenum alloys. Russ J Phys Chem 1975;49:1128-9. Available from: https://www.osti.gov/biblio/4035422 [Last accessed on 29 Jul 2022]

27. Tsai HL. Thesis, University of Tennessee, 1983.

28. Pejryd L. Experimental study of phase equilibria and thermodynamic stabilitie in the system Ni-Mo-TiO2-O, Department of Inorganic Chemistry, University of Umeå, Umeå, Sweden, 1985.

29. Pejryd L. Phase relations and stabilities in the metal-rich part of the Ni-Mo-O system in the temperature range 1200-1400 K. *Scand J Metall* 1985;14:268-272. DOI

30. Koyama K, Hashimoto Y, Suzuki K, Kameyama S. Determination of the standard gibbs free energy of formation of $NiMo_2B_2$ and the activity of the Ni-Mo binary system by EMF measurement. *J Japan Inst Metals* 1989;53:183-8. DOI

31. Wang Y, Woodward C, Zhou S, Liu Z, Chen L. Structural stability of Ni-Mo compounds from first-principles calculations. *Scripta Materialia* 2005;52:17-20. DOI

32. Zhou S, Wang Y, Jiang C, Zhu J, Chen L, Liu Z. First-principles calculations and thermodynamic modeling of the Ni-Mo system. *Mater Sci Eng* 2005;397:288-96. DOI

33. Yaqoob K, Crivello J, Joubert J. Thermodynamic modeling of the Mo-Ni system. *Calphad* 2018;62:215-22. DOI

34. Khan F, Asgar M, Nordblad P. Magnetization and magnetocrystalline anisotropy of Ni-Mo single crystal alloys. *J Magn Magn Mater* 1997;174:121-6. DOI

35. Ghosh S, Das N, Mookerjee A. Magnetic properties of Ni-Mo single-crystal alloys; theory and experiment. J Phys : Condens Matter 1998;10:11773-80. DOI

36. J.M. Dickinson, L.S. Richardson, Trans. ASM 51 (1958) 1055-1071. DOI

37. A.G. Knapton, J. Inst. Met. 87 (1958-1959) 62-64.

38. E.M. Savitskii, M.A. Tylkina, K.B. Povarova, Zh. Neorg. Khim. 1959;4:424-34.

39. E.M. Savitskii, M.A. Tylkina, K.B. Povarova, Russ. J. Inorg. Chem. 4 (1959) 190-195.

40. Farzadfar S, Levesque M, Phejar M, Joubert J. Thermodynamic assessment of the molybdenum - rhenium system. *Calphad* 2009;33:502-10. DOI

41. Kodentsov AA, Dunae SF, Slyusarenko EM, Sokolovskaya EM, Priimak AN. Phase equilibria in the rhenium-molybdenum-nickel system. Vestnik Moskovskogo Universiteta Ser.2 Khimiya, 1987;28:153-8. DOI

42. Borisov VA, Yaschenko AI, Slyusarenko EM, Dunaev SF. Moscow Univ. Chem. Bull. 1992;47:76-9.

43. Slyusarenko E, Borisov V, Sofin M, Kerimov E, Chastukhin A. Determination of phase equilibria in the system Ni-V-Cr-Mo-Re at 1425 K using the graph method. *J Alloys Compd* 1999;284:171-89. DOI

44. Feng Y. Determination of isothermal sections of the Co-Nb-Ni and Ni-Mo-Re ternary systems. *Rare Metals* 2008;27:83-8. DOI

45. Yaqoob K, Crivello JC, Joubert JM. Comparison of the site occupancies determined by combined Rietveld refinement and density functional theory calculations: example of the ternary Mo-Ni-Re σ phase. *Inorg Chem* 2012;51:3071-8. DOI PubMed

46. Chekhovskoi VY, Peletskii VE. Thermophysical properties of 75Ni-15Mo-10Re alloy. *High Temperature* 2003;41:221-8. DOI

47. Frisk K. A thermodynamic evaluation of the Mo-Ni system. *Calphad* 1990;14:311-20. DOI

48. Cui Y, Jin Z, Lu X. Experimental study and thermodynamic assessment of the Ni-Mo-Ta ternary system. *Metall Mater Trans A* 1999;30:2735-44. DOI

49. Morishita M, Koyama K, Yagi S, Zhang G. Calculated phase diagram of the Ni-Mo-B ternary system. *J Alloys Compd* 2001;314:212-8. DOI

50. Mao P, Han K, Xin Y. Thermodynamic assessment of the Mo-Re binary system. *J Alloys Compd* 2008;464:190-6. DOI

51. Mao P, Han K, Xin Y. Corrigendum to "thermodynamic assessment of the Mo-Re binary system". J Alloys Compd 2009;482:557-8. DOI

52. Yang Y, Zhang C, Chen S, Morgan D, Chang YA. First-principles calculation aided thermodynamic modeling of the Mo-Re system. *Intermetallics* 2010;18:574-81. DOI

53. Mathieu R, Dupin N, Crivello J, et al. CALPHAD description of the Mo-Re system focused on the sigma phase modeling. . *Calphad* 2013;43:18-31. DOI

54. Nash A, Nash P. Ni-Re (Nickel-Rhenium) system. *Bull Alloy Phase Diagrams* 1985;6:348-50. DOI

55. Boettinger WJ, Newbury DE, Ritchie NWM, et al. Solidification of Ni-Re peritectic alloys. *Metall Mat Trans A* 2019;50:772-88. PubMed PMC

56. Kresse G, Furthmüller J. Efficient iterative schemes for ab initio total-energy calculations using a plane-wave basis set. *Phys Rev B Condens Matter* 1996;54:11169-86. DOI PubMed

57. Dreizler RM, Gross EKU. Density functional theory. Springer Berlin Heidelberg: Berlin, Heidelberg, 1990; Chapter 4, pp 43-74. DOI

58. Kresse G, Joubert D. From ultrasoft pseudopotentials to the projector augmented-wave method. *Phys Rev B* 1999;59:1758-75. DOI

59. Perdew JP, Wang Y. Accurate and simple analytic representation of the electron-gas correlation energy. *Phys Rev B Condens Matter* 1992;45:13244-9. DOI PubMed

60. Monkhorst HJ, Pack JD. Special points for Brillouin-zone integrations. *Phys Rev* B 1976;13:5188-92. DOI

61. Blöchl PE. Projector augmented-wave method. *Phys Rev B Condens Matte*r 1994;50:17953-79. DOI PubMed

62. Zunger A, Wei S, Ferreira LG, Bernard JE. Special quasirandom structures. *Phys Rev Let*t 1990;65:353-6. DOI PubMed

63. van de Walle A, Tiwary P, de Jong M, et al. Efficient stochastic generation of special quasirandom structures. *Calphad* 2013;42:13-8. DOI

64. Shin D, Arróyave R, Liu Z, Van de Walle A. Thermodynamic properties of binary hcp solution phases from special quasirandom structures.

Phys Rev B 2006;74: 024204. DOI

65. Crivello J, Souques R, Breidi A, Bourgeois N, Joubert J. ZenGen, a tool to generate ordered configurations for systematic first-principles calculations: the Cr-Mo-Ni-Re system as a case study. *Calphad* 2015;51:233-40. DOI

66. Sundman B, Shi P. SGTE pure element database, version 5.0, Thermo-Calc Software, Stockholm.

67. Zheng W, Lu X, He Y, Cui Y, Li L. Thermodynamic assessment of the Fe-Mn-Si system and atomic mobility of its fcc phase. *J Alloys Compd* 2015;632:661-75. DOI

68. Redlich O, Kister AT. Thermodynamics of nonelectrolyte solutions - x-y-t relations in a binary system. *Ind Eng Chem* 1948;40:341-5. DOI